Study of Climate Variability and Spatio-Temporal Analysis of Sea Surface Temperature in Pacific Ocean of Nariño, Colombia: Study Period 2018–2023

Angie Paola Lozano Arias, Andrés Cárdenas Contreras

Faculty of Engineering, Cadastral and Geodesy Engineering Program
Universidad Distrital Francisco José de Caldas, Bogotá, Colombia – aplozanoa@udistrital.edu.co, acardenas@udistrital.edu.co

Keywords: Sea Surface Temperature, Climate Variability, Spatial Interpolation, Geostatistics, Kriging, Landsat Satellite Sensors

Abstract

Climate variability is one of the main challenges for coastal communities, particularly in the Colombian Pacific, where phenomena such as El Niño and La Niña significantly affect the environment and local livelihoods. This study analyzes sea surface temperature (SST) in the department of Nariño between 2018 and 2023, combining satellite imagery with local meteorological records.

Using Landsat data and IDEAM observations, spatial and temporal patterns of SST were mapped. Geostatistical methods, specifically ordinary and simple kriging, were applied to estimate temperature in areas without direct observations, with accuracy assessed through cross-validation. The results show that SST responds clearly to ENSO events, with warming during El Niño and cooling during La Niña.

Beyond technical outcomes, this work provides a practical tool to understand how ocean changes affect the region. The findings offer valuable insights for territorial planning, climate risk management, and productive sectors such as fisheries and agriculture, which depend directly on ocean dynamics.

1. Introduction

Climate change and climate variability are increasingly recognized as phenomena that not only transform the natural dynamics of ecosystems but also reshape the social and economic structures of human communities. Their impacts are particularly pronounced in coastal regions, where the direct interaction between the ocean and the atmosphere renders these territories highly sensitive. In the Colombian Pacific, the recurrent presence of large-scale phenomena such as El Niño and La Niña has historically altered water availability, agricultural productivity, and food security, directly affecting the daily lives of communities in the department of Nariño.

Within this context, Sea Surface Temperature (SST) emerges as a fundamental indicator for understanding the magnitude and direction of ocean–atmosphere interactions. SST regulates processes as relevant as evaporation, cloud formation, and precipitation patterns, and has become a critical parameter for anticipating changes in climate dynamics. Numerous international studies have demonstrated its usefulness in characterizing spatial and temporal variability and in assessing the influence of ENSO events across diverse regions of the world (Hudson & Wackernagel, 1994; Cheng et al., 2019). In Colombia, recent research has highlighted the role of SST in regional climate analysis, although most studies have focused on national scales or other areas of the country (Puertas & Carvajal, 2008; Ocampo-Marulanda et al., 2022).

Nevertheless, a gap remains in the detailed spatio-temporal analysis of SST in the Pacific region of Nariño, particularly through the application of geostatistical techniques that can more accurately model its behavior. Addressing this gap is essential not only for understanding local climate dynamics but also for generating inputs that support territorial planning, environmental management, and climate change adaptation in a region marked by high vulnerability.

To respond to this need, the present study seeks to answer the following research question: How does the spatio-temporal variability of SST behave in relation to large-scale climatic phenomena (El Niño and La Niña) in the department of Nariño between 2018 and 2023?

The general objective is to evaluate the relationship between Pacific SST anomalies and climate variability in Nariño during this period. This purpose is developed through a methodological approach that integrates satellite and hydrometeorological data with advanced statistical and geostatistical techniques, enabling the identification of spatio-temporal patterns, the fitting of spatial dependence models, and the validation of results against ENSO events recorded in the study area.

2. Data and Methods

2.1. Data and Study Area

The study area corresponds to the department of Nariño, located in southwestern Colombia with a coastline along the Pacific Ocean. This region is characterized by its climatic diversity, shaped by factors such as latitude, altitude, proximity to the coast, and the direct influence of large-scale El Niño and La Niña events. Its geographical location and oceanic exposure make Nariño a strategic territory for analyzing ocean–atmosphere interactions and their impacts on natural and social systems.

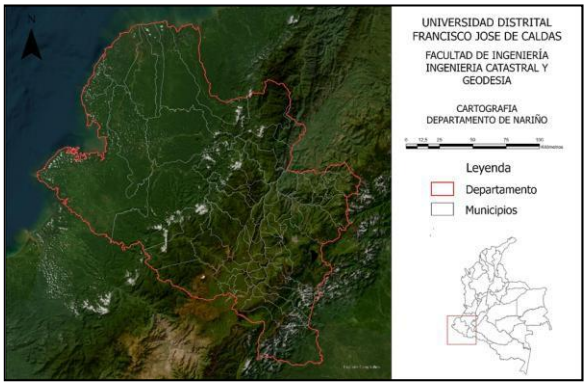

Figure 1. Study Area Location – Department of Nariño

For this research, Landsat 7, 8, and 9 satellite imagery was acquired from the United States Geological Survey (USGS), enabling the estimation of Sea Surface Temperature (SST). These images were processed in SNAP software, applying radiometric and atmospheric corrections as well as surface emissivity adjustments. In addition, hydrometeorological records from the Instituto de Hidrología, Meteorología y Estudios Ambientales (IDEAM) were incorporated, corresponding to stations within the area of influence.

Variable	Type	Source	Unit
Sea Surface Temperature	Dependent	USGS (Landsat 7, 8, 9)	°C
Relative humidity	Independent	IDEAM	%
Temperature	Independent	IDEAM	°C
Precipitation	Independent	IDEAM	mm
Solar radiation	Independent	IDEAM	h/day
Evapotranspiration	Independent	IDEAM	mm
Altitude	Independent	IDEAM	m a.s.l.
Distance to coast	Independent	IDEAM	km
Latitude	Independent	IDEAM	decimal degrees
Longitude	Independent	IDEAM	decimal degrees

Table 1. Study Variables

The variables considered included SST as the dependent variable, and as explanatory variables: relative humidity, precipitation, solar radiation, evapotranspiration, altitude, distance to the coast, latitude, longitude, and wind speed. The integration of satellite and ground-based data provided a robust database for subsequent statistical and geostatistical analysis.

2.2. Methodology

The methodology integrated satellite image processing, exploratory statistical analysis, and geostatistical modeling to characterize the spatio-temporal variability of Sea Surface Temperature (SST) in the department of Nariño during the 2018–2023 period.

2.2.1. Satellite processing and SST derivation

Landsat 7, 8, and 9 thermal images were downloaded from the United States Geological Survey (USGS). Thermal band processing was carried out in SNAP software following three stages: conversion of digital numbers (DN) to spectral radiance, transformation of radiance to brightness temperature, and correction by surface emissivity.

- Conversion from DN to spectral radiance

$$L_\lambda = M_L * Q_{cal} + A_L$$

where:

L_λ = spectral radiance ($W \cdot m^{-2} \cdot sr^{-1} \cdot \mu m^{-1}$)
M_L , A_L = calibration coefficients provided by the metadata
Q_{cal} = digital pixel value

- Radiance to brightness temperature

$$T = \frac{K_2}{\ln\left(\frac{K_1}{L_\lambda} + 1\right)}$$

where:
T = brightness temperature (Kelvin)
K_1, K_2 = Landsat thermal sensor constants

- Surface emissivity correction

$$SST = \frac{T}{1 + \left(\frac{\lambda T}{\rho}\right) \ln(\varepsilon)}$$

where:
λ = effective wavelength
$\rho = \frac{hc}{\sigma} = 1.438 * 10^{-2} m * K$
ε = surface emissivity, generally estimated using NDVI

This methodological workflow enabled the conversion of satellite imagery into a reliable, continuous SST variable expressed in degrees Celsius.

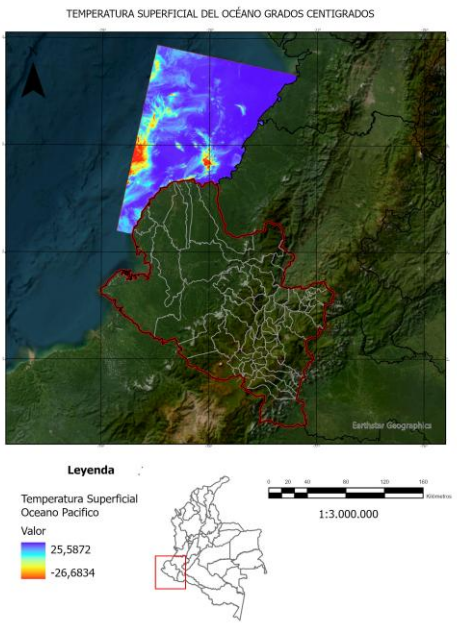

Figure 2. Final Band SST

2.2.2. Exploratory statistical analysis

The dataset was subjected to exploratory statistical analysis to assess the distribution and variability of the variables prior to spatial modeling.

First, measures of central tendency (mean, median), dispersion (variance, standard deviation, coefficient of variation), and shape (skewness and kurtosis) were calculated, which allowed for the identification of heterogeneity in SST and auxiliary variables: relative humidity, precipitation, solar radiation, evapotranspiration, altitude, latitude, longitude, distance to the coast, and wind speed.

	mean	sd	se(mean)	IQR	cv	skewness	0%	25%	50%
SST	19.5674429	2.6996820	0.22497350	1.496425	0.13796805	-1.51430483	13.084900	1.966265e+01	2.048270e+01
Alt	2054.1666667	1019.7590693	84.97992244	1298.500000	0.49643444	-0.42007334	110.000000	1.556750e+03	2.144000e+03
DistC	172.3741667	35.5941077	2.96617564	36.875000	0.20649328	-1.03648984	90.210000	1.622000e+02	1.763050e+02
Hum	78.2255103	17.6972742	1.47477285	13.136573	0.22623405	-2.02854472	9.103593	7.493289e+01	7.997059e+01
Prec	0.1508446	0.6697674	0.05581395	0.019161	4.44011557	5.62233501	0.000000	7.402401e-04	8.842517e-03
Temp	15.0842243	4.5068613	0.37557177	6.327830	0.29877978	0.49410857	6.000000	1.149464e+01	1.510871e+01
Viento	3.9012000	4.3428544	0.36190453	1.919356	1.08810744	3.00887292	1.007194	1.828180e+00	2.442500e+00
Brillos	3.4305556	1.1135075	0.09279229	2.000000	0.32458519	0.06927399	2.000000	2.000000e+00	3.000000e+00
Evapo	1001.2708333	75.7136351	6.31113625	105.750000	0.07563751	0.84753438	900.000000	9.450000e+02	9.795000e+02

	75%	100%	n
SST	2.115907e+01	22.895500	144
Alt	2.855250e+03	3585.000000	144
DistC	1.990750e+02	211.420000	144
Hum	8.806846e+01	100.000000	144
Prec	1.990124e-02	5.106343	144
Temp	1.782247e+01	26.779221	144
Viento	3.747537e+00	27.323930	144
Brillos	4.000000e+00	5.000000	144
Evapo	1.050750e+03	1192.000000	144

Figure 3. Descriptive Statistics

Second, correlations between SST and auxiliary variables were analyzed using Pearson and Spearman coefficients. This analysis showed that latitude, longitude, solar radiation, and wind speed exerted the strongest influence on SST, while precipitation and altitude played a minor role.

Finally, normality of the distributions was assessed through histograms, boxplots, QQ-plots, and hypothesis tests (Shapiro–Wilk, Kolmogorov–Smirnov). In cases of non-normality, logarithmic and Box–Cox transformations were applied to improve symmetry and stabilize variance, ensuring compliance with the assumptions required for geostatistical modeling.

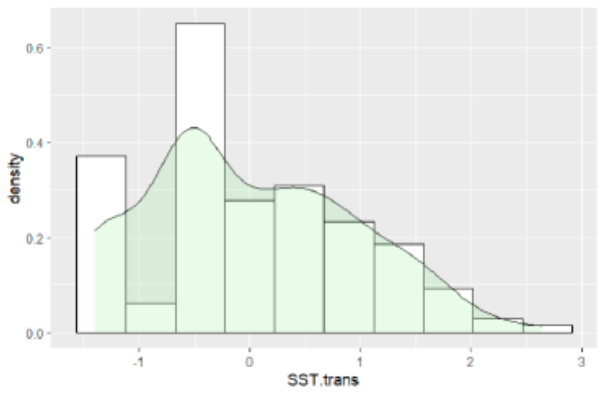

Figure 3. SST Histogram Transform

2.2.3. Geostatistical modelling

Geostatistical modeling aimed to characterize the spatial dependence of SST and generate continuous prediction maps. The process was organized into four phases: anisotropy analysis, experimental variogram construction, theoretical model fitting, and interpolation with validation.

- Anisotropy analysis

Directional variograms (0°, 45°, 90°, and 135°) were built to identify preferential directions of spatial correlation. Moderate anisotropy was detected, associated with coastal orientation and the influence of ocean currents.

- Experimental variogram

$$\gamma(h) = \frac{1}{2N(h)} \sum_{i=1}^{N(h)} [Z(x_i) - Z(x_i + h)]^2$$

where:
$\gamma(h)$= semivariance at distance
$N(h)$ = number of point pairs separated by distance
$Z(x_i)$, $Z(x_i + h)$ = SST values at locations x_i and $x_i + h$

The experimental variogram revealed short-range spatial dependence, consistent with the oceanic variability of the region.

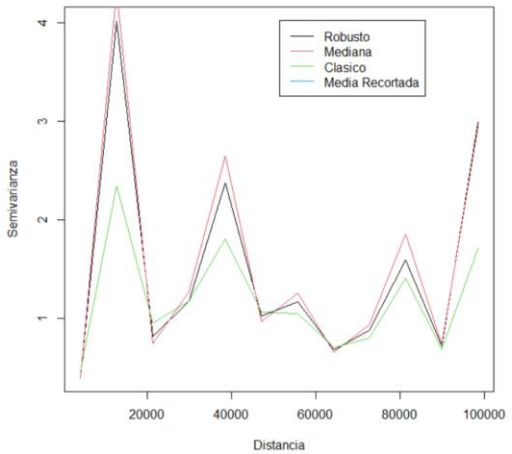

Figure 4. Semivariogram Models

- Theoretical model fitting

Spherical, exponential, and Gaussian models were evaluated. The spherical model provided the best fit, with higher R^2 and lower RMSE.

$$\gamma(h) = \begin{cases} C_0 + C\left[\frac{3h}{2a} - \frac{h^3}{2a^3}\right], 0 < h \leq a \\ C_0 + C, \quad h > a \end{cases}$$

where:
C_0 = nugget effect,
C = sill,
a = range of spatial dependence.

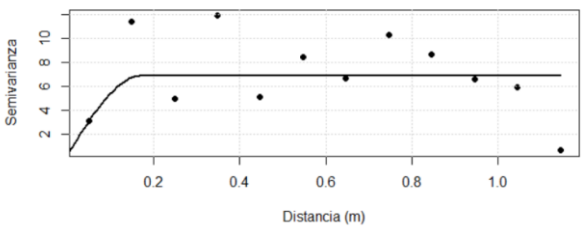

Figure 5. Spherical Variogram Modeling

- Interpolation and validation

The spatial interpolation of SST was carried out using ordinary kriging (OK) and simple kriging (SK), with the fitted spherical variogram as the spatial structure model. Additionally, Radial Basis Functions (RBF) were implemented as a non-variogram-based alternative for comparison. Interpolation and validation were performed in a sequential process, as described below.

Interpolation procedure

For each unsampled location , SST was estimated as a weighted linear combination of observed data:

$$\hat{Z}(x_0) = \sum_{j=1}^{n} w_i Z(x_i)$$

where:
$\hat{Z}(x_0)$= estimated SST at location
$Z(x_i)$ = observed SST values,
w_i = kriging weights,
n = number of neighbors within the search radius.

Two different assumptions were applied:

Ordinary kriging (OK): assumes an unknown but locally constant mean. Weights were obtained by solving the kriging system with the unbiasedness constraint:

$$\sum_{j=1}^{n} w_j = 1$$

Simple kriging (SK): assumes a known global mean m. Weights were derived from the covariance function associated with the spherical variogram:

$$C(h) = C(0) - \gamma(h)$$

The search neighborhood was defined by:

A radius equal to the range parameter a of the spherical variogram.
A maximum number of neighbors (20–30) to ensure numerical stability.
Sectorization (four quadrants) to balance the spatial distribution of neighbors.

The output consisted of:

Prediction maps of SST for both SK and OK.

Kriging variance maps $\sigma_K^2(x)$, representing uncertainty of prediction.

Validation procedure

To assess the accuracy and robustness of the interpolations, a leave-one-out cross-validation (LOOCV) scheme was applied: each observed data point was removed in turn and its value was estimated using the remaining dataset.

For each validation round, the following metrics were calculated:

- Coefficient of determination (R^2)

$$R^2 = 1 - \frac{\sum_{i=1}^{n}[Z(x_i) - \hat{Z}(x_i)]^2}{\sum_{i=1}^{n}[Z(x_i) - \bar{Z}]^2}$$

Indicates the proportion of variance in the observed data explained by the predictions. Values close to 1 denote strong predictive performance.

- Root Mean Square Error (RMSE)

$$RMSE = \sqrt{\frac{1}{n}\sum_{i=1}^{n}[Z(x_i) - \hat{Z}(x_i)]^2}$$

Measures the average magnitude of prediction errors, penalizing large deviations.

- Mean Error (ME)

$$ME = \frac{1}{n}\sum_{i=1}^{n} Z(x_i) - \hat{Z}(x_i)$$

Indicates whether the model systematically over- or underestimates SST. Values close to zero suggest unbiased predictions.

In addition to numerical indices, scatterplots of observed vs. predicted SST values were generated to visually evaluate model performance and detect potential biases at specific value ranges.

2.3. Experimental Results

The results obtained through interpolation and validation procedures allowed the characterization of the spatio-temporal variability of Sea Surface Temperature (SST) in Nariño during the 2018–2023 period.

2.3.1. SST prediction maps

The interpolated maps revealed well-defined coast–ocean gradients, with higher SST values nearshore and progressive cooling towards offshore waters. These gradients are strongly associated with solar radiation and reduced vertical mixing in shallow areas. Temporally, positive anomalies were observed during El Niño episodes (2019 and 2023), with SST up to +2 °C above the mean, while negative anomalies emerged during La Niña (2020–2021), with cooling of similar magnitude. These anomalies closely matched NOAA's Oceanic Niño Index (ONI) values for the same period.

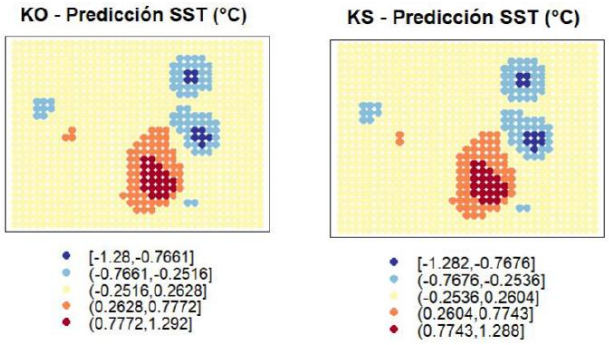

Figure 6. Interpolated SST maps: ordinary kriging and simple kriging.

2.3.2. Kriging variance maps

Kriging variance maps showed higher uncertainty offshore and in areas with sparse data, highlighting the dependence of estimation reliability on the density and distribution of reference observations. These maps provide insights not only into model performance but also into where new stations or satellite validation points should be prioritized to strengthen the monitoring network.

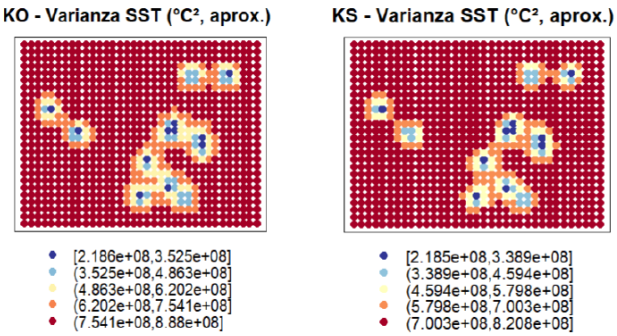

Figure 7. Kriging variance for ordinary kriging and simple kriging.

2.3.3. Cross-validation

The leave-one-out cross-validation confirmed that ordinary kriging achieved the best performance indicators, with higher R^2 and lower errors compared to simple kriging and RBF.

Method	R^2	RMSE (°C)	ME (°C)
Simple kriging (SK)	0.72	0.65	-0.08
Ordinary kriging (OK)	0.84	0.49	0.02
RBF	0.68	0.72	-0.11

Table 2. Scatterplots of observed vs. predicted SST values for: SK, OK, RBF.

Cross-validation revealed clear differences among methods:

Ordinary kriging with the spherical model achieved the best performance (R^2 = 0.84; RMSE = 0.49 °C), confirming that the mean is not homogeneous across the study area and that OK better captures gradients.

Simple kriging showed weaker performance (R^2 = 0.72; RMSE = 0.65 °C), indicating that assuming a constant mean reduces local variability modeling.

RBF was the least robust (R^2 = 0.68; RMSE = 0.72 °C), producing smoother surfaces that tended to underestimate thermal extremes.

The analysis demonstrates that SST variability in Nariño is shaped by a dual control:

- Spatial: coast–ocean gradients and north–south differences reflect the interplay of solar radiation, shallow bathymetry, and ocean circulation.
- Temporal: ENSO anomalies manifest rapidly along the coast, demonstrating the high regional sensitivity to large-scale climate forcing.

These findings imply that ocean variability cannot be understood solely as a global phenomenon but as a process that reshapes territorial dynamics at local scales. The detected patterns are key for anticipating effects on water availability, fisheries productivity, and territorial planning.

2.3.4. Radial Basis Function (RBF) Interpolation

Table 8 summarizes the performance of different Radial Basis Functions (RBFs) applied to the interpolation of Sea Surface Temperature (SST). Each model was evaluated using three key parameters: the smoothing factor (ETA), the radius of influence (Rho), and the Root Mean Square Prediction Error (RMSPE), which quantifies predictive accuracy. These metrics allow assessing each function's ability to balance fitting precision and predictive stability across the study domain.

The multiquadratic function showed intermediate performance (ETA = 0.1248; Rho = 0.0968; RMSPE = 0.1868), reflecting moderate accuracy and a stable interpolation capable of capturing overall thermal variability, though with a higher prediction error than other methods.

In contrast, the inverse multiquadratic function achieved the lowest RMSPE (0.0132), with a high ETA value (1.2799) and a nearly null Rho. This indicates a fine and stable fit with minimal dispersion between observed and predicted values. Its numerical consistency and generalization ability make it the most robust and reliable RBF for representing SST variability in the Nariño Pacific region.

Spline-type functions performed comparatively worse. Both the Tension Spline and the Completely Regularized Spline yielded similar RMSPE values (~0.2035), suggesting limited adaptability to the spatial structure of the data. The Tension Spline (Rho = 1.6495) exhibited excessive rigidity, restricting the model's flexibility in areas with abrupt temperature gradients. Meanwhile, the Completely Regularized Spline (Rho = 0.1141) reduced rigidity but without substantial improvement in accuracy.

The Thin-Plate Spline produced an exceptionally low RMSPE (0.000996), suggesting an almost perfect fit. However, such a result likely indicates overfitting, where the model adheres too closely to observed data, reducing its predictive capability in

regions with sparse sampling or highly variable oceanic conditions.

Overall, despite the Thin-Plate Spline's minimal numerical error, the Inverse Multiquadratic function stands out as the most balanced and reliable RBF, combining high accuracy, numerical stability, and strong generalization performance.

Radial Basis Function	ETA	Rho	RMSPE
Multiquadratic	1.25×10^{-1}	9.68×10^{-2}	1.87×10^{-1}
Inverse Multiquadratic	1.28×10^{0}	7.93×10^{-8}	1.32×10^{-2}
Tension Spline	1.00×10^{-21}	1.65×10^{0}	2.03×10^{-1}
Completely Regularized Spline	1.00×10^{-21}	1.14×10^{-1}	2.03×10^{-1}
Thin-Plate Spline	9.97×10^{-4}	0.00×10^{0}	9.97×10^{-4}

2.4. Discussion

The results obtained for Nariño's Pacific coast are consistent with documented ENSO-related SST responses in tropical oceans, showing warming during El Niño and cooling during La Niña (Cheng et al., 2019; Puertas & Carvajal, 2008; Ocampo-Marulanda et al., 2022). Unlike broader-scale analyses that average over large areas, this study provides a fine-scale quantification that resolves coastal gradients and short-range dependencies. This contribution addresses a persistent gap in Colombian coastal research, where SST variability has traditionally been analyzed from sparse, station-based datasets with limited spatial representativeness.

From a methodological perspective, ordinary kriging with a spherical variogram model outperformed simple kriging and radial basis functions, confirming previous findings that emphasize its robustness when the mean cannot be assumed constant across the study area (Hudson & Wackernagel, 1994; Isaaks & Srivastava, 1989; Cressie, 1993). The use of kriging variance maps added an explicit quantification of uncertainty—an element rarely reported in regional SST studies but essential for guiding future observation and interpolation strategies.

The association of SST with latitude, longitude, solar radiation, and wind speed aligns with physical–statistical frameworks that highlight the control of radiative forcing and surface mixing on oceanic temperature patterns (Holdaway, 1996; Cheng et al., 2019). Conversely, precipitation, humidity, and altitude exhibited minor influence, reaffirming that coastal SST variability responds primarily to continuous energy gradients rather than episodic atmospheric events.

Beyond confirming these spatial relationships, the geostatistical analysis revealed isotropic behavior and a short practical range (~0.15), indicating that spatial autocorrelation decays rapidly with distance. This implies that effective monitoring of nearshore thermal variability requires high-density observation networks to capture short-range processes accurately. Strengthening the local network with automatic sensors and oceanographic buoys—complementing IDEAM's terrestrial stations—would enable continuous monitoring and early warning systems for ENSO-related thermal anomalies.

Scientifically, this research demonstrates the potential of combining remote sensing and geostatistics to model ocean–atmosphere coupling in tropical coastal environments. The methodological framework developed here provides a replicable approach that integrates Landsat imagery and IDEAM data, bridging spatial modeling with local meteorological information. Future studies should extend this framework toward spatio-temporal models, incorporating dynamic variables such as surface currents, solar radiation, and salinity, and leveraging multi-sensor datasets from MODIS, Sentinel-3, or VIIRS to enhance temporal continuity and predictive capacity.

At the applied level, the findings offer a valuable technical foundation for territorial planning, environmental management, and climate adaptation in the Colombian Pacific. Identifying areas of anomalous warming or cooling can inform fisheries management, coastal agriculture planning, and marine ecosystem conservation. Ultimately, the study confirms that SST variability is a tangible expression of ocean–atmosphere coupling, where energy gradients, radiation, and wind dynamics act as key drivers of local climate behavior. Understanding these mechanisms is critical to anticipate ENSO impacts and support evidence-based decision-making for resilient and sustainable coastal development.

3. Conclusions

The analysis of Sea Surface Temperature (SST) in the Pacific coast of Nariño during the 2018–2023 period provided a comprehensive understanding of the interaction between oceanic and atmospheric processes governing regional climate variability in southwestern Colombia. The spatio-temporal characterization revealed two distinct thermal regimes—a warm regime (19–21 °C) and a cold one (13–15 °C)—closely associated with the alternating phases of the El Niño–Southern Oscillation (ENSO). This pattern confirms the ocean's modulating role on coastal climate and its influence on continental thermal stability.

The most influential factors controlling SST distribution were latitude, longitude, distance from the coast, wind speed, solar radiation, and evapotranspiration, representing energy transfer and vertical mixing mechanisms that shape coastal ocean dynamics. In contrast, precipitation, relative humidity, and altitude had marginal effects, suggesting that SST variability is driven primarily by continuous energetic gradients rather than episodic atmospheric phenomena.

Geostatistical modeling confirmed isotropic behavior and validated the spherical variogram model, with a low nugget, a sill near 6, and a short practical range (~0.15). These results indicate that spatial autocorrelation decays rapidly with distance, emphasizing the importance of maintaining high-density observation networks to accurately capture short-range thermal variability. Among the interpolation techniques, ordinary kriging achieved the best performance, complemented by simple kriging and radial basis functions (RBF), which provided versatility and stability in thermally heterogeneous areas.

From a scientific perspective, this study reinforces the value of geostatistics and remote sensing as integrative tools for representing marine thermal variability. The proposed methodological framework is replicable and adaptable to future research on ocean–atmosphere interactions in tropical regions. From an applied standpoint, the findings offer a valuable technical basis for territorial planning, environmental management, and climate adaptation in the Colombian Pacific, particularly in fisheries and coastal agriculture. Understanding the mechanisms that modulate SST enables better anticipation of ENSO impacts and global warming trends, contributing to science-based and sustainable decision-making.

References

Burrough, P.A. & McDonnell, R.A., 1998. Principles of Geographical Information Systems. Oxford University Press, New York.

Cheng, L., Abraham, J., Hausfather, Z. & Trenberth, K.E., 2019. How fast are the oceans warming? Science, 363(6423), pp.128–129.

Cressie, N., 1993. Statistics for Spatial Data. Wiley, New York.

Goovaerts, P., 1997. Geostatistics for Natural Resources Evaluation. Oxford University Press, New York.

Holdaway, M.R., 1996. Spatial modeling and interpolation of monthly temperature using kriging. Climate Research, 6(3), pp.215–225.

Hudson, G. & Wackernagel, H., 1994. Mapping temperature using kriging with external drift: theory and an example from Scotland. International Journal of Climatology, 14(1), pp.77–91.

IDEAM, 2022. Reportes hidrometeorológicos para Colombia. Instituto de Hidrología, Meteorología y Estudios Ambientales. Available at: https://www.ideam.gov.co/ (Accessed: 10 June 2024).

Isaaks, E.H. & Srivastava, R.M., 1989. An Introduction to Applied Geostatistics. Oxford University Press, New York.

Journel, A.G. & Huijbregts, C.J., 1978. Mining Geostatistics. Academic Press, London.

NOAA, 2023. Oceanic Niño Index (ONI). National Oceanic and Atmospheric Administration. Available at: https://origin.cpc.ncep.noaa.gov/products/analysis_monitoring/ensostuff/ONI_v5.php (Accessed: 15 July 2024).

Oliver, M.A. & Webster, R., 2015. Basic steps in geostatistics: the variogram and kriging. SpringerBriefs in Agriculture. Springer, New York.

Ocampo-Marulanda, J., Rojas, D.A. & Carvajal, Y., 2022. Variabilidad climática y océano en el Pacífico colombiano. Revista de Climatología y Geociencias, 42(2), pp.45–60.

Puertas, M. & Carvajal, Y., 2008. Efectos de El Niño en la dinámica oceánica del Pacífico sur colombiano. Revista Colombiana de Geografía, 17, pp.89–102.

USGS, 2023. Landsat Collection 2 Level-2 Science Products. U.S. Geological Survey. Available at: https://landsat.usgs.gov/ (Accessed: 20 July 2024).